# The identity of the AB1 and NE4 electron paramagnetic resonance spectra in high-pressure–high-temperature diamond

## W Gehlhoff[1] and R N Pereira[2]

Institute of Solid State Physics, Technical University Berlin, PN5-2, Hardenbergstr. 36,
D-10623 Berlin, Germany

E-mail: gehlhoff@sol.physik.tu-berlin.de

## Abstract

Similar electron paramagnetic resonance (EPR) spectra caused by the trigonal centres NE4 and AB1 have been detected in nitrogen-rich diamond synthesized with Ni catalyst by two different groups. The NE4 centre is commonly considered to be the basic structure of several nickel–nitrogen centres that are formed upon the annealing of this type of diamond. However, its EPR spectrum is observed so far only in diamond crystals grown in Novosibirsk, whereas in similar crystals grown in the NIRIM the AB1 centre could be detected. This discrepancy in the EPR detection could be solved by a re-analysis of the published EPR data of the NE4 centre and through EPR investigations of synthetic diamonds from Novosibirsk and the NIRIM. The study revealed that the EPR spectrum of the NE4 centre corresponds in fact to the spectrum of the trigonal AB1 centre, which is described with $S = 1/2$ and the $g$-values $g_\parallel = 2.0027 \pm 0.0002$ and $g_\perp = 2.0923 \pm 0.0002$. Furthermore, we study whether the experimental $g$-values can be successfully explained, within the framework of crystal-field theory, by the previously proposed models for the AB1 (NE4) centre.

## 1. Introduction

The unique physical properties of diamond and the substantial success of high-pressure–high-temperature (HPHT) synthesis of diamond using transition metal solvent/catalysts make this material very attractive for numerous applications, from electronic to mechanical purposes. Depending on the growth conditions and the solvent/catalysts used, these synthetic diamond crystals contain various types of impurity-related defect, that can significantly alter their

[1] Author to whom any correspondence should be addressed.
[2] On leave from: The Department of Physics, University of Aveiro, 3810 Aveiro, Portugal.

properties. Therefore, considerable effort is addressed to identify and characterize the different centres found in as-grown and annealed diamonds. The most common of these, nitrogen, is known to be present in isolated substitutional sites, either in the paramagnetic neutral state ($N_S^0$: P1 electron paramagnetic resonance (EPR) centre [1, 2]) or positively charged diamagnetic state [3], and also in aggregated forms (*A* and *B* aggregates [30]), especially after annealing of the crystals. When Ni or Ni alloys are used as solvent catalysts, Ni is incorporated into the diamond lattice in the form of dispersed atoms, giving rise to several EPR and optical spectra. The relative intensities of these signals are dependent on the nitrogen concentration in the sample. Diamonds with higher nitrogen content (>50 ppm) exhibit typically optical centres with zero-phonon lines (ZPLs) at 1.885 and 2.5 eV [4]. Besides, the well known P1 centre and the single substitutional nickel $Ni_S^-$, which gives rise to the EPR line at $g = 2.0319$ (W8 EPR centre with spin $S = 3/2$ [5]), are also observed. Furthermore, several paramagnetic defects with strong evidence of nickel participation have been found by EPR in recent years [6–13]. Among these centres the AB1–AB6 [6–8] and NE1–NE8 [13] defects are detected in nitrogen-rich crystals, whereas in samples with low nitrogen concentration from the National Institute for Research in Inorganic Materials (NIRIM), Japan, the centres NIRIM1, NIRIM2 [8–10] and AB7 [8, 9] are observed. A comparison of the results published for as-grown and annealed nitrogen-rich HPHT diamonds evidences essential discrepancies in the occurrence of some centres in diamonds of different origins. In particular, the NE4 spectrum, originally detected in crystals grown in Novosibirsk [11, 12], was never reported to be observed in as-grown or annealed HPHT diamonds from NIRIM. The NE4 spectrum is generally assumed to originate in a defect that is the common structure of the nickel–nitrogen complexes, which are formed during high-temperature heat treatments [13]. The NIRIM samples are grown through a similar method as used in Novosibirsk [15], using Ni-containing solvent/catalysts. In addition, the nickel–nitrogen complexes NE1–NE3 and NE5 have frequently been detected in the NIRIM samples [6–8]. Moreover, the NIRIM crystals seem to exhibit the same behaviour upon annealing [9], regarding the formation of the Ni–N complexes, as that originally reported for the diamond samples grown in Novosibirsk [13]. In the reverse case, the AB1–AB6 centres have been detected in as-grown and annealed NIRIM samples rich in nitrogen, and to the best of our knowledge were never reported by other groups which have been working on HPHT diamonds synthesized in Novosibirsk [13, 15]. These apparent differences in the formation of Ni-related centres in diamond may be actually caused by a shift of the Fermi level due to intentional or unintentional incorporation of other impurities or due to changes in the impurity concentrations, and/or can be caused by peculiarities of the growth processes. Such discrepancy in the appearance of defects makes the comparison of optical and magnetic resonance data and the study of the mechanisms of formation of the different centres more complicated.

The present article is directed towards finding the reasons for the discrepancy regarding the detection of the NE4 and AB1 EPR spectra in diamond.

## 2. Experimental details

Two synthetic diamonds grown in a multianvil split-sphere ultrahigh-pressure apparatus with an iron–nickel solvent/catalyst system at temperatures and pressures in the region of 1750 K and 5.5–6.0 GPa [15], respectively, were used in order to verify the EPR parameters of the NE4 spectrum. The diamond crystals show an octahedral growth habit and are light yellow in colour. Infrared absorption measurements indicate that the samples contain both P1 centres and nitrogen aggregates with a somewhat inhomogeneous concentration distribution in the region of about 120 and 2.5 ppm, respectively. From EPR measurements, the concentration of $Ni_S^-$ (W8) was estimated to be between 4 and 8 ppm. The EPR linewidth of the P1 transitions

(0.17 mT) corresponds to a centre concentration of about 150 ppm [16]. This indicates that the local density of $N_S^0$ in some regions was somewhat larger than indicated by the average EPR intensity and IR absorption.

The main crystallographic directions of the samples were aligned with respect to the external magnetic field $B$ through the use of the growth facets checked by x-rays. Measurements were made with the applied $B$ field rotated in a $\{110\}$ plane, where all principal high-symmetry directions can be accessed. The precise orientation of the crystal relative to the applied magnetic field $B$ was tested using the well documented P1 spectrum with its highly isotropic $g$-value ($g_\parallel = 2.0024$ and $g_\perp = 2.0025$ [2]) and the well resolved anisotropic hyperfine structure from its 99.63% abundant $^{14}$N isotope with nuclear spin $I = 1$ [1, 18], reflecting a $\langle 111 \rangle$-relaxed position of the atom [17]. However, owing to the small trigonal hyperfine anisotropy, with constants (in units of $10^{-4}$ cm$^{-1}$) $A_\parallel = 38.04$ and $A_\perp = 27.13$ [18] and the linewidth of 0.17 mT, the accuracy of the determination of the rotation axis is not better than $\pm 0.5°$.

EPR measurements were carried out on a Bruker ESP 300E spectrometer mounted with an X-band microwave bridge. To avoid the cutting of the rather large available samples (about 0.9 ct), the standard equipment, comprising an Oxford Instruments helium gas flow cryostat (ESR 900) with the matched cylindrical or rectangular cavity, was replaced by a helium bath cryostat with a dielectric ring TE$_{011}$ cavity. Besides, due to the appreciable increase of the filling factor and the enhancement of the magnetic component of the microwave field at the sample the sensitivity of the spectrometer increases especially in studies of non-saturable samples.

Microwave frequencies and magnetic fields were measured with a Hewlett-Packard 5352B counter and a Bruker ER035M digital gaussmeter, respectively. The highly isotropic electronic $g$-value of the P1 centre was used to correct the small difference between the magnetic field experienced by the sample and that measured by the gaussmeter probe.

## 3. Results and discussion

### 3.1. Re-analysis of the published data

The NE4 EPR spectrum was first detected by Nadolinny *et al* [11, 12] in as-grown and annealed synthetic diamond grown under the conditions described in [15]. In figure 1, the previously reported angular dependence of the line positions of the NE4 spectrum is shown. This variation corresponds to the rotation of the magnetic field in a $\{110\}$ plane and was obtained by digitizing the data shown in figure 2 of [12]. The data were described using the spin Hamiltonian

$$H = \beta B \cdot g \cdot S, \tag{1}$$

with $S = 1/2$ and the $g$-matrix with parameters $g_\parallel$ and $g_\perp$ for the four possible centre orientations of a trigonal centre in a cubic (tetrahedral) crystal. The authors determined the following parameters: $g_\parallel = 2.0227$ ($B \parallel \langle 111 \rangle$) and $g_\perp = 2.0988$ [11, 12]. Assuming that the experimental line positions around $B$ perpendicular to the centre axis and the given $g_\perp$ value are correct, the value of the microwave frequency used in the experiment described in [12] was estimated here to be $f = 9.2850$ GHz. A calculation of the angular position of the line positions using the given $g$-values and $f = 9.2850$ GHz reveals a considerable discrepancy to the experimental points (see figure 1), which is presumably caused by a misleading determination of the experimental line position for $B \parallel \langle 111 \rangle$. An inspection of figure 2 in [12] clearly shows that both parameters were merely determined from the line positions corresponding to the centre orientations for which $B$ becomes parallel or perpendicular to the trigonal centre axis during
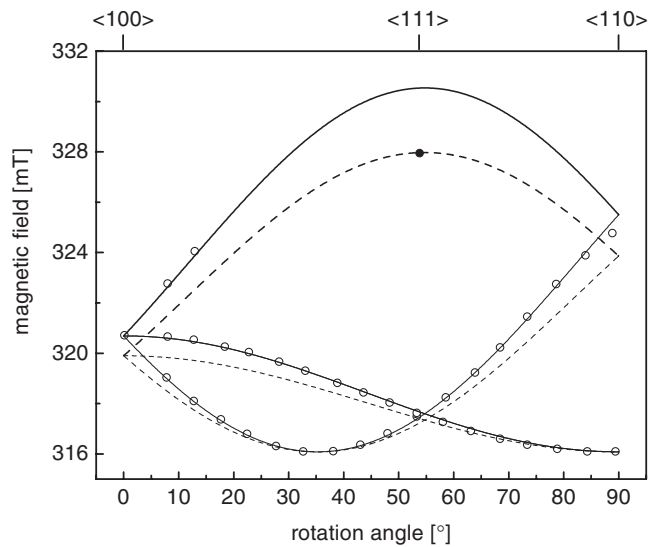
**Figure 1.** Comparison of the experimental EPR line positions of the trigonal NE4 centre taken from [12] (presented as open or solid circles) for a rotation of the magnetic field $B$ in a $\{110\}$ crystallographic plane with those calculated using equation (1) and assuming a microwave frequency of $f = 9.2850$ GHz (see the text): (dashed curves) using the published $g$-parameters $g_\parallel = 2.0227$, $g_\perp = 2.0988$ [11, 12], and (solid curves) using the parameters $g_\parallel = 2.007$ and $g_\perp = 2.0988$.

the complete rotation in a $\{110\}$ plane. Although the experimental points given in the figure in [12] are connected with lines, they cannot be calculated using the spin Hamiltonian (1) with the given $g$-values. Due to the strong overlapping with the EPR lines of the P1 and W8 centres, the authors could not follow the angular dependence of the NE4 EPR spectrum above 325 mT, which corresponds to $B$ orientations deviating from the $\langle 111 \rangle$ direction by less than $\pm 35°$. It is likely that for $B \parallel \langle 111 \rangle$ a weak signal from another centre was erroneously identified as belonging to the NE4 spectrum (this line is represented as a solid point in figure 1). If we remove this single point for $B \parallel \langle 111 \rangle$ and calculate the complete angular dependence with equation (1) and $f = 9.2850$ GHz, we obtain a rather good agreement with the experimental points using the $g$-values $g_\parallel = 2.007$ and $g_\perp = 2.0988$. Besides, the analysis of figure 1 in [12], where the spectra of the P1, W8 and NE4 are shown for $B \parallel \langle 100 \rangle$, reveals that the line positions of the P1 and W8 centres do not correspond to their well known $g$-values. From the P1 lines of figure 1 in [12] we determine the microwave frequency used to measure the spectrum to be $f = 9.2609$ GHz. Using this frequency value we obtain from the data shown in figure 1 the $g$-values $g_\parallel = 2.0018$ and $g_\perp = 2.0934$ for the NE4 centre. Both this set of values and the set $g_\parallel = 2.007$ and $g_\perp = 2.0988$ are considerably close to the $g$-values found for the AB1 centre: $g_\parallel = 2.0024 \pm 0.0002$ and $g_\perp = 2.0920 \pm 0.0002$ [7]. This re-analysis of the published data strongly suggests that the correct spin Hamiltonian parameters of the NE4 centre are identical to those given for the AB1 defect [7].

### 3.2. New experimental results

To examine whether the NE4 and AB1 spectra really result from the same centre we measured EPR on the above-mentioned samples grown in Novosibirsk [15]. The P1 and W8 centres cause the dominant EPR signals in these samples. However, optimizing the measurement conditions
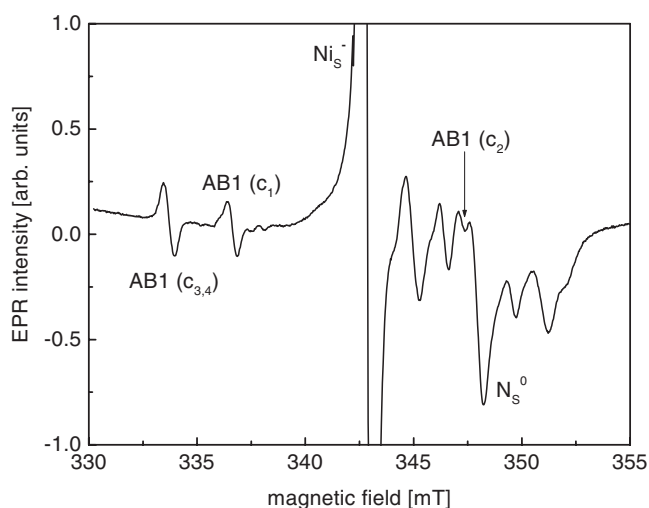
**Figure 2.** X-band ($f = 9.7507$ GHz) EPR spectrum of an as-grown diamond sample from Novosibirsk for $B \parallel \langle 100 \rangle + 66°$ in a $\{110\}$ crystal plane, obtained at $T = 110$ K and high microwave power.

it is possible to detect besides some weaker signals the signal from the trigonal AB1 centre with moderate intensity. Figure 2 shows a typical EPR spectrum of the samples obtained for $B \parallel \langle 100 \rangle + 66°$ in a $\{110\}$ plane. As a result of the high microwave power used for optimizing the AB1 signal, the transitions of the P1 centre are partly saturated and therefore the lines are broadened and their lineshape is distorted. The different saturation behaviour of the AB1 and P1 centres upon the microwave power and temperature could be successfully used to determine the AB1 line positions in the magnetic field region where this spectrum overlaps with the very strong unsaturated P1 lines. The complete angular dependence of the AB1 line positions for the rotation in a $\{110\}$ plane is shown in figure 3. The $g$-values $g_\parallel = 2.0027 \pm 0.0002$ ($B \parallel \langle 111 \rangle$) and $g_\perp = 2.0923 \pm 0.0002$ give the best fit of equation (1) to the experimental line positions. These values are in very good agreement with the values previously determined in Q-band measurements [7]. Since other characteristics of the observed spectrum are also the same, like the linewidth and saturation behaviour, it is established that the NE4 and AB1 spectra have their origin in the same paramagnetic defect.

### 3.3. Assignment of the AB1 (NE4) centre to optical spectra

The identification of the NE4 spectrum as being the same as the AB1 centre spectrum questions also the tentative assignment of the doublet structure at 1.72 eV to the NE4 spectrum, that was proposed by optical detection of electron paramagnetic resonance (ODEPR) investigations via the magnetic circular dichroism (MCDA) [19]. This assignment was assumed to be the most probable despite the fact that the deviation between the measured $g_\parallel$ values was not within the experimental error. However, the possibility that the EPR spectrum observed was a new $Ni^+$ defect with a structure similar to that of the NE4 centre was not ruled out by the authors [19]. The comparison of the $g$-values of the AB1 centre with the values $g_\parallel = 2.004 \pm 0.005$ ($B \parallel \langle 111 \rangle$) and $g_\perp = 2.093 \pm 0.005$ determined from the angular dependence of the ODMR measurements [19] provides evidence that the AB1 data fit the ODEPR angular dependence much better, as was recently suggested [7]. The results presented here clearly corroborate the
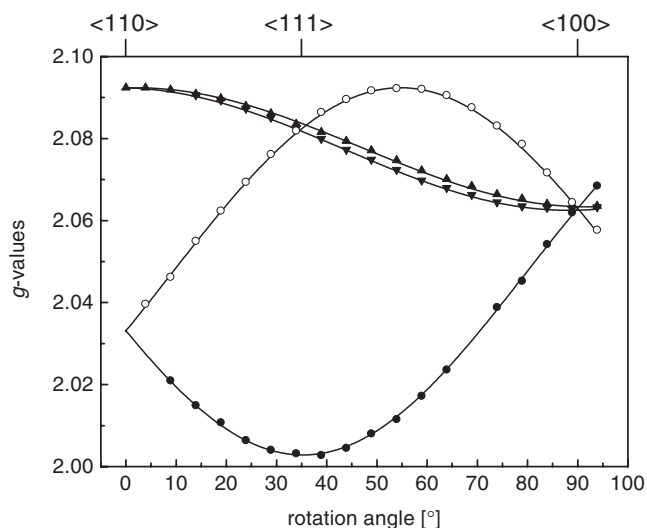
**Figure 3.** Angular dependence of the AB1 (NE4) EPR lines for rotation of the magnetic field $B$ in a slightly misaligned {110} crystal plane. The symbols represent the experimental data for the four centre orientations and the solid curves are the angular dependences calculated using the fitted values $g_\parallel = 2.0027$, $g_\perp = 2.0923$. The line splitting ($\blacktriangle$, $\blacktriangledown$) between both centre orientations perpendicular to the rotation plane is caused by a small misorientation of the $\langle 110 \rangle$-rotation axis of $\Delta\theta = 0.3°$, $\Delta\phi = 1.2°$ ($\langle 1.0207, 0.9788, 0.0074 \rangle$).

assignment of the 1.72 eV MCDA doublet to the paramagnetic AB1 (NE4) centre. The NE4 EPR spectrum was tentatively assigned to the 1.40 eV optical system [20]. However, more recent experiments seem to indicate that the latter optical feature is indeed connected with the NIRIM2 EPR centre [19, 21].

### 3.4. The models for the AB1 (NE4) centre

There are some proposed structures for the AB1 (NE4) centre consistent with its symmetry and electronic spin $S = 1/2$, as well as other properties of the EPR spectrum like the rather small linewidth of the detected transitions and the behaviour of the nickel-related centres upon heat treatments. For instance, it was originally proposed that the NE4 spectrum arises from $Ni^+$ ($3d^9$) positioned in the centre of a double semivacancy site oriented along a $\langle 111 \rangle$ direction [11]. This model did not consider the covalent bonding with the surrounding atoms. More recently, it was argued that this defect is formed by one Ni ion in the trigonally distorted strong octahedral field of the double semivacancy site, with a $d^5$ ($t_2^5$) configuration due to the six covalent bonds with its nearest-neighbour carbon atoms: $(C_3VNiVC_3)^-$ [13]. This model corresponds to the microscopic structure of the tin-vacancy pair in silicon first described by Watkins [22]. Such structure is considered to be the basic fragment unit of the variety of nickel–nitrogen centres which are generated upon heat treating nitrogen-rich diamonds grown from nickel solvent/catalysts [13].

Moreover, a substitutional $Ni_S^+$ ($3d^9$ configuration with free ion $LS$-term $^2D$) associated with a carbon vacancy in an $\langle 111 \rangle$ direction and a nickel ion (probably also with $3d^9$ configuration) in interstitial site with a trigonal distortion produced by a next-nearest-neighbour vacancy $(Ni_iC–V)^+$ were suggested as probable models for NE4 [19] and AB1 EPR spectra [23], respectively. If the substitutional nickel forms four covalent bonds with its neighbours, the

former model corresponds to a complex $(\text{Ni}_S\text{C–V})^{3-}$. The assumption of such a configuration is not unrealistic, since recent *ab initio* electronic structure calculations, using the Green function linear muffin-tin orbital method in the atomic-sphere approximation (LMTO-ASA), have shown that the threefold negative state of substitutional nickel in diamond is likely to be stable [29].

Although a definitive choice between these and other speculative models for the AB1 (NE4) centre should be based on the (as yet unavailable) hyperfine and ligand-hyperfine interactions, and be corroborated by *ab initio* calculations, some deduction of its nature can be obtained from the interpretation of the available data in the framework of the simple crystal-field theory. Two of the mentioned models, $\text{Ni}^+$ in the position between two empty lattice sites [11] and interstitial $\text{Ni}_i$ with an adjacent carbon vacancy $(\text{Ni}_i\text{C–V})^+$ [23], may be assumed as being a $^2\text{D}$ state (single hole) in a trigonally distorted cubic crystal field. The crystal-field theory of the energy levels and $g$-factors of a single 3d electron (or hole) at a trigonally distorted tetrahedrally or octahedrally coordinated site is well developed [24–26]. In the presence of the cubic crystal field produced by the covalent charge distribution on the ligand atoms, the $^2\text{D}$ state splits into the doubly degenerate $^2\text{E}$ and triply degenerate $^2\text{T}_2$ orbital states, with the $^2\text{E}$ state being lowest in energy for a dominant octahedral crystal field. Previous studies of interstitial nickel in diamond [21] assume a level ordering similar to that observed in silicon, where the octahedral crystal field from the next-nearest neighbours is dominant over the tetrahedral field of the nearest neighbours [27]. Assuming in our case the same behaviour of $\text{Ni}^+$ in the trigonally distorted interstitial site, then both models predict a $^2\text{E}$ ground state. In contrast to a tetragonal crystal-field distortion, a trigonal field causes no splitting of the $^2\text{E}$ ground state. However, the simultaneous presence of the trigonal field and the spin–orbit coupling between the ground ($^2\text{E}$) and excited ($^2\text{T}_2$) states produces a second-order splitting of the $^2\text{E}$ ground state into a pair of Kramers doublets: $\Gamma_4$ and $\Gamma_{5,6}$ [24, 26]. The principal $g$-factors calculated for both ground state doublets $\Gamma_{5,6}$ and $\Gamma_4$ are [21, 26]

$$g_\parallel(\Gamma_{5,6}) = 2 - \frac{4\lambda'k'}{\Delta_c} - \frac{8k'K'}{\Delta_c} \qquad \text{and} \qquad g_\perp(\Gamma_{5,6}) = 0,$$

$$g_\parallel(\Gamma_4) = 2 - \frac{4\lambda'k'}{\Delta_c} + \frac{8k'K'}{\Delta_c} \qquad \text{and} \qquad g_\perp(\Gamma_4) = \frac{4\lambda'k'}{\Delta_c}, \tag{2}$$

where $\Delta_c$ is the cubic crystal-field splitting between the $^2\text{E}$ and $^2\text{T}_2$ states. The primed parameters $\delta'$, $\lambda'$ and $k'$, which couple $^2\text{E}$ to $^2\text{T}_2$, are the trigonal crystal-field splitting, the spin–orbit coupling parameter and an orbital reduction factor, respectively. Both doublet states can be excluded as explanations of the experimental $g$-values $g_\parallel = 2.0027$ and $g_\perp = 2.0923$, because for the $\Gamma_{5,6}$ states $g_\perp$ should be zero and for the $\Gamma_4$ state the experimental $g$-values can be realized only for the completely unrealistic parameters $\Delta_c \cong 2\lambda'k' = 4\delta'k'$.

For the model of substitutional $\text{Ni}_S^+$ (3d$^9$, de$^4$ dt$^5$) associated with a carbon vacancy in a $\langle 111 \rangle$ direction a $^2\text{D}$ free ion ground state also results. However, since it experiences a cubic crystal field of opposite sign, the ordering of the E and $\text{T}_2$ levels is inverted. The ground state $\text{T}_2$ is split by the trigonal crystal field and the spin–orbit coupling into three doublet states: $2 \times \Gamma_4(\text{T}_2)$ and $\Gamma_{5,6}(\text{T}_2)$. If we omit corrections from the coupling to the $^2\text{E}$ excited state, the $g$-factors for the lower $\Gamma_4$ state (regardless of the sign of the trigonal crystal-field distortion) are given by [21]

$$g_\parallel = 2(a^2 - b^2) - 2kb^2, \qquad g_\perp = 2a^2 + 2\sqrt{2}kab, \tag{3}$$

with

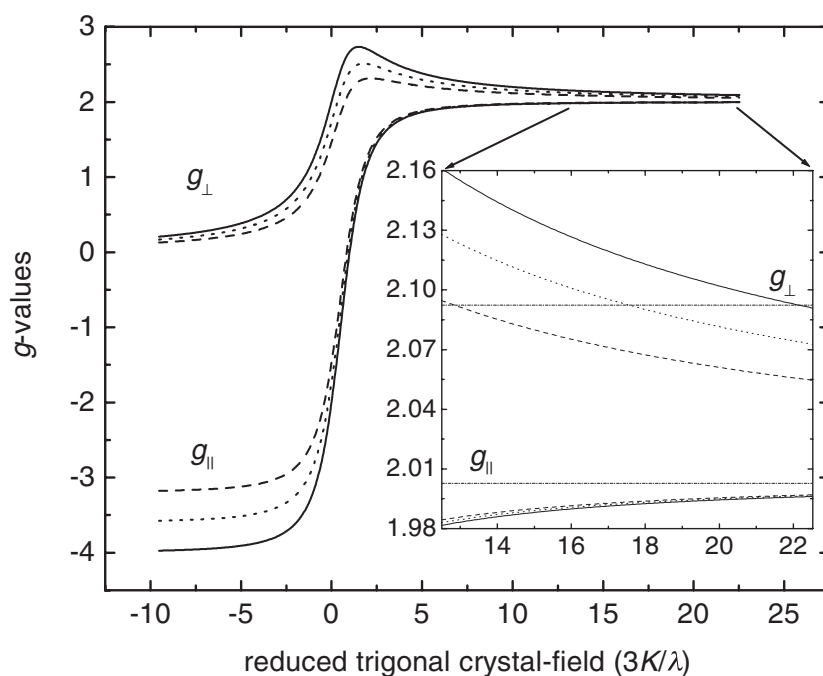$$a = \cos\alpha, \qquad b = \sin\alpha, \tag{4}$$

**Figure 4.** Plot of the g-values $g_\parallel$ and $g_\perp$ against the reduced trigonal crystal field $(3K/\lambda)$ for a $^2T_2$ state resulting from a $d^9$ configuration in a nearly tetrahedral environment for different orbital quenching factors $k$. Contributions from the excited $^2E$ state and outside the $^2E + {}^2T_2$ manifold are ignored. Appropriate for a single $d^9$ hole the spin–orbit parameter $\lambda$ has been taken to be negative.

and

$$\tan 2\alpha = \frac{\sqrt{2}\lambda}{3K - \frac{\lambda}{2}}, \tag{5}$$

where $\lambda$ and $K$ are the spin–orbit coupling parameter and one-third of the crystal-field splitting within the $^2T_2$ state, respectively. The possible g-values $g_\parallel$ and $g_\perp$ are shown in figure 4 as a plot of the reduced trigonal field splitting $(3K/\lambda)$, where the spin–orbit parameter $\lambda$ appropriate for a single $d^9$ hole has been taken to be negative. For orbital quenching factors $k$ in the range 0.6–1.0, the $g_\perp$ value can be fitted for reduced trigonal field values $(3K/\lambda)$ between 13 and 22, whereas $g_\parallel$ is always slightly smaller (0.82–0.33%) than the spin-only value 2.0023 for such values, in contradiction with the experimental results. The corrections from the coupling to the $^2E$ excited state can increase the $g_\perp$ values for some values of the reduced trigonal field. However, there is no improvement of the fitting for reliable coupling parameters, as the $g_\parallel$ values that are then calculated are always slightly reduced. In this approach, which considers only interaction within the two-dimensional manifold, a better fit of the experimental parameters can only be obtained for very small values of the reduced trigonal field. However, again such values of the trigonal field are also unrealistic for the considered model of substitutional nickel associated with a carbon vacancy.

Standard crystal-field theory also predicts a $^2T_2$ ground state for the $(C_3VNiVC_3)^-$ model, which corresponds to a $d^5$ $(t_{2g}^5)$ configuration in a trigonally distorted strong octahedral field. The $t_{2g}^5$ configuration can be considered in the one-electron approximation as a single hole

in an otherwise filled d shell. If we neglect admixture with the $^2E$ and other states, the $^2T_2$ ground state will have the same splitting behaviour and the same $g$-factors (equations (3)–(5)) as the above-considered case of a $d^9$ ion in a trigonally distorted tetrahedral crystal field. Since the $d^5$ configuration contains altogether ten states belonging to the $^2T_2$ representation, excited states will be mixed, changing the magnetic properties of the ground state if the octahedral crystal field is not extremely strong. For completely octahedral symmetry, it was shown that admixtures from the $t_{2g}^4 e_g$ excited configuration can in particular contribute significantly to the magnetic properties of the $^2T_2$ ground state by increasing the $g$-values of the ground doublet by a few per cent [28]. Such admixtures can possibly explain the small discrepancies between the experimental and theoretical $g$-values of the AB1 centre within the simple crystal-field approach. This issue merits further studies, which are, however, beyond the scope of the present article.

## 4. Conclusions

The EPR spectrum of the trigonal NE4 centre, which has been observed in as-grown and annealed synthetic HPHT diamond crystals grown by the split-sphere technique [15] by Nadolinny *et al* [11, 12], was never detected in as-grown and annealed HPHT diamond samples synthesized at the NIRIM [9]. A re-analysis of the published data has led to a more accurate determination of the spin Hamiltonian parameters describing the anisotropy of the NE4 EPR spectrum. The analysis clearly indicates that the latter spectrum is in fact due to the trigonal AB1 centre. Such inference could be confirmed by EPR studies of synthetic diamonds with the same origin as the crystals at which the NE4 EPR spectrum has been detected. The proof of the identity of the AB1 and NE4 centres also corroborates the proposed assignment of the doublet of lines at 1.72 eV found by ODEPR (MCDA) investigations to AB1 paramagnetic defects. The calculation of the $g$-values within the framework of crystal-field theory shows that among the proposed models for the AB1 (NE4) centre only the models of a nickel ion at the centre of the double semivacancy $(C_3VNiVC_3)^-$ with a $d^5$ $(t_{2g}^5)$ configuration in a trigonal distorted strong octahedral field and of substitutional nickel $Ni_S^+$ $(3d^9)$ with an associated defect (vacancy or an impurity ion) can explain the experimental $g$-values.

## Acknowledgments

## References

[1] Smith W V, Sorokin P P, Gelles I L and Lasher G J 1959 *Phys. Rev.* **115** 1546
[2] Zhang S, Ke S C, Zvanut M E, Tohver H T and Vohra Y K 1994 *Phys. Rev.* B **49** 15392
[3] Lawson S C, Fisher D, Hunt D C and Newton M E 1998 *J. Phys.: Condens. Matter* **10** 6171
[4] Lawson S C and Kanda H 1993 *J. Appl. Phys.* **73** 3967
[5] Isoya J, Kanda H, Norris J R, Tang J and Bowman M K 1990 *Phys. Rev.* B **41** 3905
[6] Neves A J, Pereira R N, Sobolev N A, Nazaré M H, Gehlhoff W, Naeser A and Kanda H 1999 *Physica* B **273/274** 651
[7] Neves A J, Pereira R N, Sobolev N A, Nazaré M H, Gehlhoff W, Naeser A and Kanda H 2000 *Diamond Relat. Mater.* **9** 1057
[8] Pereira R N, Neves A J, Gehlhoff W, Sobolev N A, Rino L and Kanda H 2002 *Diamond Relat. Mater.* **11** 623
[9] Pereira R N, Gehlhoff W, Neves A J, Sobolev N A and Kanda H 2002 to be published
[10] Isoya J, Kanda H and Uchida Y 1990 *Phys. Rev.* B **42** 9843

[11] Nadolinny V A and Yelisseyev A P 1994 *Diamond Relat. Mater.* **3** 1196
[12] Nadolinny V A, Yelisseyev A P, Yuryeva O P and Feygelson B N 1997 *Appl. Magn. Reson.* **12** 543
[13] Nadolinny V A, Yelisseyev A P, Baker J M, Newton M E, Twitchen D J, Lawson S C, Yuryeva O P and Feygelson B N 1999 *J. Phys.: Condens. Matter* **11** 7357
[14] Nadolinny V A, Yelisseyev A P, Baker J M, Twitchen D J, Newton M E, Feigelson B N and Yuryeva O P 2000 *Diamond Relat. Mater.* **9** 883
[15] Polyanov Yu N, Malinovsky I Yu, Borzdov Yu M, Khokhryanov A F, Chepurov A I, Godovikov A A and Sobolev N V 1990 *Dokl. Akad. Nauk SSSR* **315** 1221 (Engl. transl. 1991 *Sov. Phys.–Dokl.* **35** 324)
[16] van Wyk A, Reynhard E C, High G L and Kiflawi I 1992 *J. Phys. D: Appl. Phys.* **30** 8119
[17] Breuer S J and Briddon P R 1996 *Phys. Rev.* B **53** 7819
[18] *Landolt–Börnstein New Series* 2002 Group III vol 41, ed O Madelung, U Roessler and M Schulz (Berlin: Springer)
[19] Pawlik Th, Noble C and Spaeth J-M 1998 *J. Phys.: Condens. Matter* **10** 9833
[20] Nadolinny V A and Yelisseyev A P 1994 *Diamond Relat. Mater.* **3** 1196
[21] Mason P W, Ham F S and Watkins G D 1999 *Phys. Rev.* B **60** 5417
[22] Watkins G D 1975 *Phys. Rev.* B **12** 4383
[23] Baker J M, Nadolinny V A, Newton M E and Twitchen D J 2002 *Diamond Conf. (Cambridge, 2000)* unpublished
[24] Dietz R E, Kamimura H, Sturge M D and Yaric A 1963 *Phys. Rev.* **132** 1559
[25] Scherz U 1969 *J. Phys. Chem. Solids* **30** 2077
[26] Kaufmann B, Dörnen A and Ham F S 1997 *Phys. Rev.* B **55** 13009
[27] Ludwig G W and Woodbury H H 1962 *Solid State Physics* vol 13, ed F Seitz and D Turnbull (New York: Academic) p 223
[28] Thornley J H M 1968 *J. Phys. C: Solid State Phys.* **1** 1024
[29] Overhof H and Gerstmann U 2001 private communication
[30] Davies G 1999 *Physica* B **273/274** 15